

Allosteric propagation of curvature along filament

KEN SEKIMOTO^{1,2}

¹ *Laboratoire Gulliver, UMR CNRS 7083, ESPCI Paris, Université PSL
10 rue Vauquelin, 75005, Paris, France.*

² *Laboratoire Matière et Systèmes Complexes, UMR CNRS 7057, Université Paris Cité,
10 Rue Alice Domon et Léonie Duquet, 75013, Paris, France*

Abstract – Can a filament transmit the curvatures across the constituting modules and control them at one of its end? Inspired by the observation of protofilament — constituent biopolymer of microtubule — this question is addressed by a constructive approach. In our model a simple allosteric element in each module couples with the neighboring modules at its interfaces, which gives rise to a single degree of freedom to control the global shape of the filament. The model can be analyzed in analogy with discrete-time dynamical systems having a bifurcation of trans-critical type.

Introduction. – One dimensional assemblies of identical modules can exhibit various intrinsic structures such as circle, spiral or helix apart from thermal fluctuations. Those structures are unique when the constituting module is rigid and the connection at the interface is inflexible. The protofilament, a linear assembly of tubulin dimers as constituting modules, has shown a wide distribution of curvature from sample to sample when the protofilaments are isolated, either as subcritical nucleus of a microtubule (oligomer) [1] or as the terminal part of the plus end of a microtubule [2].

From the point of view of the mechanics with constraints, the above observations motivates us to design the possible mechanism by which the linear association of identical modules realises the propagation of the curvature whose magnitude is tuneable. To simplify the problem, we limit ourselves to the two dimensional curves as the global shape of the filament, excluding twist or helix. Also we ignore thermal fluctuations and flexibility except for free joints that constitute the elements of each module. The requirement is that the system can be extend by appending the module in the way that the system has always a single “shape variable” in a continuous domain. For these purposes it is clear that each module should bear at least one internal degree of freedom and that such freedom should correlate allosterically the interface between the neighboring modules. In fact a study of structural biologists [3] suggests the correlation between the conformational change of the module interface and the curvature¹. Below we construct a toy model to verify the possibility of the above idea and examen the properties of the model.

The organisation of the paper is as follows: In §**Real toy model** we present a macroscopic construction by real wooden pieces and some bolts and nuts for demonstration of feasibility

of the idea. Then in §**Numerical model** we introduce a mathematical model for the module (§§*Module and Interfaces*), and define how the modules are connected (§§*Linkage and Dynamical System*). Next, we present the results of numerical studies for some selected cases §§*Case studies* and then develop a more general view in terms of the discrete-time dynamical system in §§*Normal form*. The final section §*Discussion* is a summary and discussion.

Real toy model. – The real physical modelling helps our intuition on the one hand but also serves as a feasibility check of the local three-dimensional arrangement of real objects. An implicit constraint is that the module should not be too sophisticated nor powered or controlled by some external source.

Our starting idea is to couple the two interfaces of a module through an allosteric mechanism. We know that the shearing of a square box \square inclines its vertical sides on its left and right, if the edges are connected by free joints. In order to make incline the vertical sides in the opposite orientations, we may revise the square box to make a twisted box \boxtimes . To make propagate such an anti-correlated inclination, we conceived a toy whose module consists of the elements shown in Fig.1(a). We call the pieces $B^- A^- A^+ B^+$ and $C^- C^+$ the backbone and shaft, respectively. The three-dimensional architecture of the pieces is schematised in a perspective view, Fig.1(b), where we took as the reference state the straight conformation. If we assign the index i for each module from the root ($i = 0$) towards the plus end ($i = m$) of the chain, the joints in Fig.1(b) can be represented as

$$\begin{aligned} A_i^+ &= A_{i+1}^-, & (i = 0, \dots, m-1), \\ B_i^+ &= C_{i+1}^+, & B_i^- = C_{i-1}^-, & (i = 1, \dots, m-1) \end{aligned} \quad (1)$$

where, for example, A_i^+ is the element A^+ of the i -th module. In the context of the growing phase of biofilament, the index

¹See Fig.2c of [3]

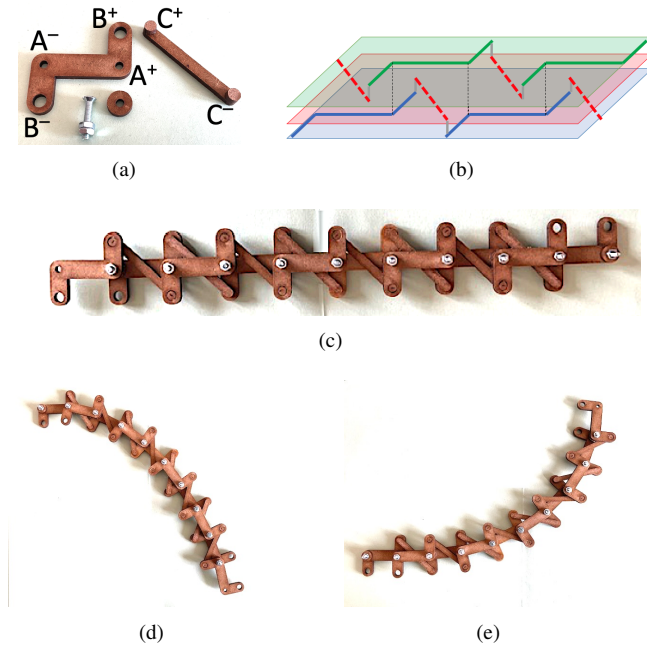


Fig. 1: (a) Constitutive elements of the module used in the toy model. The Z-shaped “backbone” $B^-A^-A^+B^+$ and straight “shaft” C^+C^- define the module, which are connected as described below. The ring, bolt and nut assure the free articulation at A^\mp . The distance between A^- and A^+ is 30mm. (b) Perspective view of the 3D design of the toy model. The structure is drawn in the reference (straight) state. The backbone elements (thick lines) are alternatively laid in the top and bottom layers, while only the shafts (dashed lines) are found in middle layer. The vertical lines traversing multiple layers indicate the free joints. (c) The model realized in the reference straight conformation. Convex (d) and concave (e) conformations.

i would also mean the temporal order of modular attachment. Fig.1(c) shows the realisation of these connections in the reference state with $m = 9$.²

In handling this chain-like object, we can verify that the system has (ideally) only a single continuous degree of freedom. In short the present architecture, therefore, can make the curvature propagate. Figs.1(d) and 1(e) show, respectively, examples of convex and concave conformations. We will discuss the details in §Numerical model in more general context.

Numerical model. –

Module and Interfaces. We characterise the shape of the backbone by the four real parameters, (f, ϕ_0, n, ν_0) , as depicted in Fig.2(a), where the central edge A^-A^+ is supposed to be of unit length. The interfaces with the neighbour modules are formed, as shown by the shaded regions in Fig.2(b). The length of the shaft is *not* the independent parameter but determined through the definition of the reference configuration, see below.

Linkage and Dynamical System. The allosteric propagation of curvature through the filament is realised through the matching condition at the interfaces of modules. We impose that the aforementioned conditions (1) are satisfied by the

²We think that the alternation of the layers of backbone is avoidable by realising the joint $A_{i-1}^+A_i^-$ in a single plane.

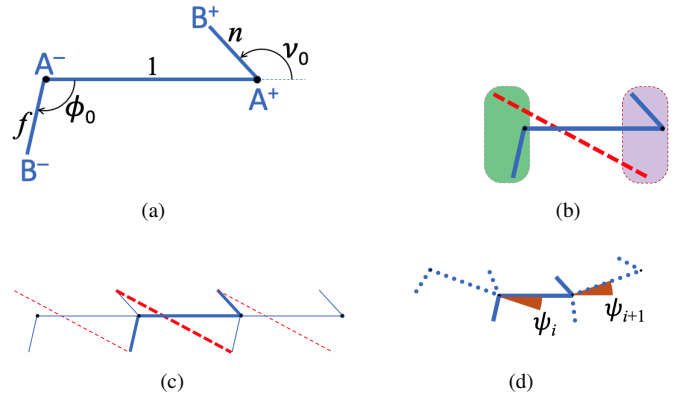


Fig. 2: (a) Backbone of each module and its parameterisation relative to the “vertebrate,” A^-A^+ , of unit length. (The backbone in Fig.1(a) corresponds to the case of $f = n = 1/2$ and $\nu_0 = \phi_0 = \pi/2$.) (b) Backbone (solid lines) and shaft (dashed line) define two interfaces (shaded zones). (c) Determination of the length of shaft, L_0 , (the thick dashed line) through the matching condition of the interfaces in the reference conformation. (d) Assignment of the flexion angles. These angles are tightly connected through (3) in the main text.

straight conformation. The length of the shaft L_0 then obeys,

$$L_0 = \left\| \begin{pmatrix} 1 \\ 0 \end{pmatrix} + f \begin{pmatrix} \cos(-\phi_0) \\ \sin(-\phi_0) \end{pmatrix} - n \begin{pmatrix} \cos(\nu_0) \\ \sin(\nu_0) \end{pmatrix} \right\|, \quad (2)$$

where $\|\cdot\|$ is the module of the vector, see Fig.2(c).

Once the dimensions of elements are defined, we count the number of freedom of the toy model, for example, shown in Fig.1(c). There we see the eight shafts that constrain the nine flexion angles along the ten backbone elements. We, therefore, have a single $(9-8=1)$ continuous degree of freedom. To see how the flexion angles are constrained iteratively, we denote by ψ_i the flexion angle at the i -th joint, see Fig.2(d). Then the second line of (1) under the fixed length L_0 of the shaft imposes the relation including ψ_i and ψ_{i+1} for $i = 0, 1, \dots, m-1$:

$$\left\| \begin{pmatrix} 1 \\ 0 \end{pmatrix} + f \begin{pmatrix} \cos(-\phi_0 + \psi_{i+1}) \\ \sin(-\phi_0 + \psi_{i+1}) \end{pmatrix} - n \begin{pmatrix} \cos(\nu_0 - \psi_i) \\ \sin(\nu_0 - \psi_i) \end{pmatrix} \right\| = L_0. \quad (3)$$

The last equation implicitly defines a dynamical system,

$$\psi_{i+1} = \Phi(\psi_i), \quad (4)$$

with the fictive discrete time, i .

Case studies. Despite the fact that the modules are identical along the linear chain, the sequence $\{\psi_i\}$ generated by (3) is in general non-constant except for the trivial fixed point, $\psi_i = 0$ for $\forall i$. For example, we tested the evolution with $f = n = 1/2$. We found that when $\{\phi_0, \nu_0\} = \{\pi/2, 7\pi/12\}$ or $\{7\pi/12, \pi/2\}$, the only non-trivial fixed point is $\psi_i = \pi/12$, while under $\{\phi_0, \nu_0\} = \{\pi/2, 5\pi/12\}$ or $\{5\pi/12, \pi/2\}$, the only non-trivial fixed point is $\psi_i = -\pi/12$. When the initial angle deviates from these fixed point values, the deviation of ψ_i either decreases (Fig.3(a)) or increases (Fig.3(b)) with i from the root to the tip. As dynamical system the underlying return map (4) exhibits the *transcritical* type of bifurcation, which is schematized in Fig.4, see, for example, [4]. What we have studied in §Real toy model belongs to the critical case, as depicted

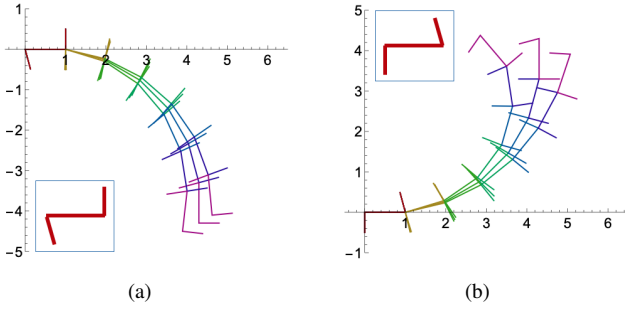


Fig. 3: Numerically calculated profiles with the flexion angles ψ_i being in the vicinity of the fixed points of Eq.(4). The shafts are not shown. Among the three profiles shown in (a) and (b) the middle ones are of the fixed-point evolution. The insets show the shape of backbone studied with $f = n = 1/2$ and (a) $\{\phi_0, \nu_0\} = \{5\pi/12, \pi/2\}$ or (b) $\{\phi_0, \nu_0\} = \{\pi/2, 7\pi/12\}$.

in Figs.4(b) and 4(e). In fact, Figs.1(d) and 1(e) show the cases starting from $\psi_0 < 0$ and of $\psi_0 > 0$, respectively, and the evolution that follows showed the monotonous decrement and increment of absolute curvature, in accordance with the critical return map Fig.4(e).³

Normal form. The normal form of the trans-critical type (the relevant term near the critical point) is given,

$$\psi_{i+1} = \psi_i - \lambda\psi_i(\mu - \psi_i) \quad (5)$$

with $\lambda > 0$. See Fig.4(g). The presence of the critical point $\mu = 0$ is a robust nature of this bifurcation, where the stable and unstable branches of fixed point crosses transversally. Having a single control parameter, μ , implies that the four-dimensional shape space $\{f, \phi_0, n, \nu_0\}$ is divided into two domains separated by a three-dimensional manifold corresponding to the critical point $\mu = 0$, which we will denote by the equation, $\Lambda(f, \phi_0, n, \nu_0) = 0$.

We can formally construct this manifold by noticing the identity, $\Lambda(f, \phi_0, f, \pi - \phi_0) = 0$, telling us that any backbone with point-inversion symmetry realises the critical bifurcation system ($\mu = 0$), see Fig.4(e), where $(\psi_i, \psi_{i+1}) = (0, 0)$ is the doubly degenerated fixed point. The above identity stems from the following equivalence relationship in (3),

$$\Leftrightarrow \begin{cases} \{\psi_i\}_{0 \leq i \leq m-1} \text{ with } \{f, \phi_0, n, \nu_0\} \\ \{-\psi_{n-i}\}_{0 \leq i \leq m-1} \text{ with } \{n, \pi - \nu_0, f, \pi - \phi_0\}, \end{cases} \quad (6)$$

where the stable fixed point is mapped into the unstable one and vice versa⁴. Then $\Lambda(f, \phi_0, f, \pi - \phi_0) = 0$ defines a two-dimensional sub-manifold of the critical manifold in the shape space. The former sub-manifold can be lifted to the latter manifold by solving $\Lambda(f, \phi_0, n, \nu_0) = 0$ as a relation between n and ν_0 passing through $(n, \nu_0) = (f, \pi - \phi_0)$.

Discussion. – We have presented a possible designing framework of statically propagating the curvature along an ex-

³In the real toy model the conformations contain errors since the physical joints are not completely tight.

⁴Since the filament generally has polarity, we distinguish a conformation and its mirror or point-inversion images in the 2D plane of the previous figures.

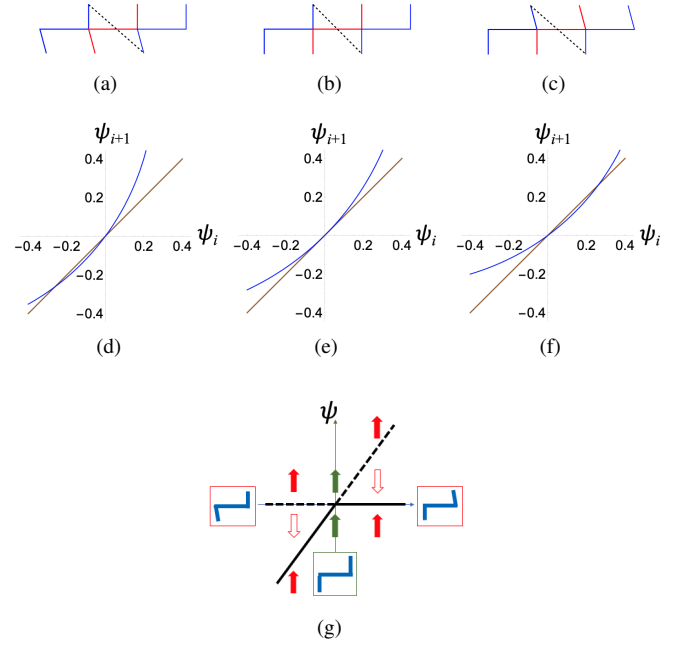


Fig. 4: Modular structure of backbone and shaft (dashed lines) in the reference state with (a) $(\phi_0, \nu_0) = (5\pi/12, \pi/2)$ realising a non-zero stable fixed point, $\psi = -\pi/12$, (b) $(\phi_0, \nu_0) = (\pi/2, \pi/2)$ realising the marginal critical point, $\psi = 0$, and (c) $(\phi_0, \nu_0) = (\pi/2, 7\pi/12)$ realising the unstable fixed point, $\psi = \pi/12$, where $f = n = 1/2$ in all cases. (d)-(f): The return maps, $\psi_i \mapsto \psi_{i+1}$, with the backbones shown above (a)-(c), respectively. (g) Schematic diagram of the trans-critical bifurcation whose normal form is given by Eq. (5). The horizontal axis represents the bifurcation parameter, μ , while the vertical direction represents the flexion angle ψ with the arrows indicating the (discrete) flow from ψ_i to ψ_{i+1} . The solid [dashed] lines represent, respectively, the stable [unstable] fixed points. The origin ($\mu = \psi_i = 0$) is the marginally stable fixed point. The boxes indicate the correspondence between the return maps in Fig.4 and the sign of μ .

tensible chain of identical modules. The geometrical constraints imposed by the internal element (“shaft”) of each module leaves only a “shape variable”, the unique continuous degree of freedom that controls the global conformation of the filament. We note that this freedom, a kind of zero-mode, does not need any fine tuning: For example, if the shape parameters ϕ_0, ν_0 and L_0 are replaced, respectively, by the local ones ϕ_i, ν_i and L_i , the modified return map, $\psi_{i+1} = \Phi_i(\psi_i)$ like (4) being adapted mutatis mutandis, will still allows the curvature to propagate. In real systems such a zero-mode will have finite persistence length due to the elastic deformability and thermal noise acting on the constituting elements of the module. The architecture shown in Fig.1 may remind us of the “Ultra-Hand”⁵, an adjustable reach extender whose unique shape variable controls the affine extension of pantographs connected in series.

It is evidently far-fetched to expect that the present toy model gives some direct relevance to the states and growth of real biopolymers. We should be content, however, if some of the

⁵The “Ultra-Hand” is a toy invented by Gunpei Yokoi of Nintendo (1966, Japan), see Wikipedia: <https://en.wikipedia.org/wiki/Ultra-Hand>

aspects we have observed in the study of this model were to reveal certain universal features. This study brought us at least two conclusions: First, the geometrical construction imposes in general a non-uniform flexion/curvature except for some special angle of flexion. Secondly, if the modules are identical, the return map (4) can have non-trivial fixed point corresponding to a circular arc-shaped with specific curvature.

We have described the shaft of each module (Fig.1) as an allosteric agent that transmit the information of an interface to the other through the body of the module. From the viewpoint of the constrained mechanics, however, this can be regarded as a non-local mechanical coupling between the backbones of next nearest neighbours. Such structure reminds us of the epaxial muscles of a snake that are reported to have interlinked attachment sites [5]. While the shafts having fixed length serve to propagate the curvature through the zero-mode, the muscles of snake can vary the local curvature in space and time through their contraction.

* * *

The author thanks *Fablab* of Université Paris Cité for letting him to use their laser cutter to make the real toy model, and Olivier Marande for the technical suggestions and assistance. He thanks Etsuko Muto for critical comments. He also thanks Muhittin Mungan for reading the draft.

REFERENCES

- [1] AYUKAWA R., IWATA S., IMAI H., KAMIMURA S., HAYASHI M., NGO K. X., MINOURA I., UCHIMURA S., MAKINO T., SHIROUZU M., SHIGEMATSU H., SEKIMOTO K., GIGANT B. and MUTO E., *Journal of Cell Biology*, **220** (2021) e202007033.
- [2] MCINTOSH J., O'TOOLE E., MORGAN G., AUSTIN J., ULYANOV E., ATAULLAKHANOV F. and GUDIMCHUK N., *Journal of Cell Biology*, **217** (2018) 2691.
- [3] RAVELLI R., GIGANT B., CURMI P., JOURDAIN I., LACHKAR S., SOBEL A. and KNOSSOW M., *Nature*, **428** (2004) 198.
- [4] GUCKENHEIMER J. and HOLMES P., *Nonlinear oscillations, dynamical systems, and bifurcations of vector fields (§3.4)* 7th Edition no. 42 in *Applied mathematical sciences* (Springer, New York) 2002.
- [5] PENNING D. A., *Journal of Anatomy*, **232** (2018) 1016.